and have linked them to reaction patterns.

Acknowledgment. This work was supported by a grant from the National Science Foundation, No. CHE-79-23204. The authors also acknowledge the purchase of an inert-atmosphere drybox by the Research Corporation. Discussions with R. G. Bergman and D. J. Darensbourg were especially helpful.

Registry No. $Li^+CpMo(CO)_3^-$, 68550-41-4; $Na^+CpMo(CO)_3^-$, 12107-35-6; $K^+CpMo(CO)_3^{3-}$, 62866-01-7; $PPN^+CpMo(CO)_3^-$, 67486-18-4; $Li^+CpCr(CO)_3^-$, 48121-51-3; $Na^+CpCr(CO)_3^-$, 12203-12-2; $K^+CpCr(CO)_3^-$, 69661-90-1; $Li^+CpW(CO)_3^-$, 80662-55-1; $Na^+CpW(CO)_3^-$, 12107-36-7; $K^+CpW(CO)_3^-$, 62866-03-9; HMPA, 1608-26-0; *n*-BuI, 542-69-8; *n*-BuBr, 109-65-9; BzlCl, 100-44-7; BzlBr, 100-39-0; $CpMo(CO)_3CH_2Ph$, 12194-07-9.

Energy Surfaces in the Cyclopropane Radical Ion and the Photoelectron Spectrum of Cyclopropane

J. R. Collins and G. A. Gallup*

Contribution from the Department of Chemistry, University of Nebraska—Lincoln, Lincoln, Nebraska 68588. *Received May 15, 1981*

Abstract: We have performed calculations to determine the two lowest energy surfaces of the cyclopropane radical cation. These are degenerate at a number of geometries, including, of course, arrangements with D_{3h} symmetry. We have used a method we call targeted correlation. This is a flexible procedure allowing us to tailor wave functions to a particular problem by treating the electron correlation in selected regions of a molecule accurately, while using more economical descriptions in other parts of the molecule. The lower surface shows a relatively flat pseudorotation region with three symmetrically equivalent saddle points of one type, three symmetrically equivalent saddle points of another type, and six symmetrically equivalent minima. The three-membered carbon ring is a scalene triangle at each of the minima. The total change in the energy along the pseudorotation path is approximately 0.3 eV. The upper surface does not show a pseudorotation region but has three relatively deep, symmetrically equivalent minima which correspond to an open-ring trimethylene radical ion isomer. Our calculations give a difference of 1.3 eV between the upper energy and the lower energy minima. When this result is combined with our calculated energy for neutral cyclopropane, we estimate 9.8 and 11.1 eV for the adiabatic onset positions of the first two peaks in the PES of cyclopropane. These compare very well with experiment. A more complex description of the PES peak profile is also offered.

Cyclopropane is a very important substance for theoretical study since it incorporates in one small molecule many physical and chemical phenomena and provides opportunities for intercomparisons. When represented by the Walsh model,[1] C_3H_6 has both Hückel and Mobius[2] orbital systems. It may also be considered the smallest aromatic system.[3] C_3H_6 has also been studied by many experimental techniques. Among these is the photoelectron spectrum (PES), which has been determined for C_3H_6[4] and many substituted versions.[5] The understanding of the substituent effects on the PES depends on an understanding of the PES of the parent compound.

The several theoretical studies of $C_3H_6^+$ have used semiempirical methods and have attempted to determine the parameters of the surfaces from calculations restricted to C_{2v} geometries for which the C_3 triangle is always at least isosceles.[6] The most involved analysis is that of Rowland who uses Koopmann's theorem and closed-shell CNDO calculations of the parent C_3H_6 to estimate functional dependence of the Jahn-Teller surfaces for the ion up to quadratic terms and then does a vibronic analysis to get the band profile. He finds a double-peaked distribution of vibrational intensities with a separation of 0.37 eV, a value three times too small.

In this article we describe the results of our ab initio calculations giving portions of the first two energy surfaces of $C_3H_6^+$, the final state in the PES. We have extended the calculations to C_s geometries where the C_3 triangle is scalene. These results provide some new insight into the details of these energy surfaces relating them to various chemically interesting bonding patterns. We also discuss the relationship between these energy surfaces and the vibronic coupling which ultimately determines the vibrational structure of the ion and the profile of the PES peak.

Details of the Calculations

To obtain the $C_3H_6^+$ energy surfaces we have used the method of *targeted correlation*[7] which is described elsewhere. Since we are, in this case, principally interested in the dependence of the energy upon the geometry of the C_3 triangle, this provides a useful simplification by allowing a more accurate treatment of the correlation in the C–C bonds than in the C–H bonds. In line with this we consider no geometries in which the C–H distances are significantly distorted from the equilibrium value.

For $C_3H_6^+$ we assemble the targeted correlation wave function from SCF orbitals for three separate methylene fragments. It is possible to orient CH_2 so that the ground state is $^3B_2$ in C_{2v} symmetry. The ground configuration is then $(1a_1)^2(2a_1)^2(1b_1)^2(3a_1)(1b_2)$, and we have determined these by a conventional open-shell Roothaan SCF procedure[8] using 3G STOs[9] as the AO basis. These orbitals were determined as a function of the H–C–H

(1) A. D. Walsh, *Nature (London)*, **159**, 712 (1947); *Trans. Faraday Soc.*, **45**, 179 (1949).
(2) M. D. Harmony, S. N. Mathur, J. Choe, M. Kattija-Ari, A. E. Howard, and S. W. Staley, *J. Am. Chem. Soc.*, **103**, 2961 (1981).
(3) M. J. S. Dewar, *Bull. Soc. Chim. Belg.*, **88**, 957 (1979).
(4) "Molecular Photoelectron Spectroscopy", D. W. Turner, Ed., Wiley-Interscience, New York, 1970, p 203 ff.
(5) T. Bally, E. Haselbach, and Z. Lanyiova, *Helv. Chim. Acta*, **61**, 2488 (1978); see also ref 4.
(6) E. Haselbach, *Chem. Phys. Lett.*, **7**, 428 (1970); C. G. Rowland, *ibid.*, **9**, 169 (1971); P. Bischof, *Croat. Chem. Acta*, **53**, 51 (1980); J. A. Tossell, J. H. Moore, and M. A. Coplan, *Chem. Phys. Lett.*, **67**, 356 (1979); S. Beran and R. Zahradnik, *Collect. Czech. Chem. Commun.*, **41**, 2303 (1976).
(7) R. L. Vance and G. A. Gallup, *Chem. Phys. Lett.*, in press.
(8) C. J. J. Roothaan, *Rev. Mod. Phys.*, **32**, 179 (1960).
(9) W. J. Hehre, R. F. Stewart, and J. A. Pople, *J. Chem. Phys.*, **51**, 2657 (1969).

0002-7863/82/1504-1530$01.25/0

angle for use in the $C_3H_6^+$ ion at the correct geometry. Examination of the orbitals shows clearly that the $2a_1$ and $1b_1$ orbitals are principally the C–H bonds, with the $3a_1$ orbital having relatively little involvement in the bonding.

We now assemble the wave function for $C_3H_6^+$ from the molecular orbitals of the three CH_2 fragments which we label A, B, and C. With 15 orbitals and 23 electrons the Weyl dimension formula[10] tells us there are 127 400 doublet functions possible for all configurations. Most of these have little chemical significance, and we consider only those with the constant doubly occupied portion for 18 of the electrons. This leaves five (six for C_3H_6)

$$(1a_{1A})^2(1a_{1B})^2(1a_{1C})^2(2a_{1A})^2(2a_{1B})^2(2a_{1C})^2(1b_{1A})^2(1b_{1B})^2(1b_{1C})^2$$

electrons to be distributed among the six orbitals $3a_{1A}$, $3a_{1B}$, $3a_{1C}$, $1b_{2A}$, $1b_{2B}$, and $1b_{2C}$. If the three CH_2 fragments are oriented so that their H atoms are symmetrically placed above and below the C_3 plane, then we get 210 $^2A'$ (175 $^1A'$ for C_3H_6) functions. These give a full CI with respect to this subset of all the orbitals. For our calculations we actually used a slightly smaller set of functions which is obtained by eliminating double charge exchange configurations. This leaves 198 (159 for C_3H_6) functions in the CI. Tests show these restrictions affect the energies by less than 0.002 eV.

Description of the Energy Surfaces

We have determined the energies for a large number of geometries of $C_3H_6^+$. For all these the symmetry is at least C_s, with the reflection plane containing the three carbon atoms. At some points the symmetry is higher, C_{2v} or even D_{3h}. The ground state of $C_3H_6^+$ shows a pronounced pseudorotation structure, and we use pseudorotation coordinates[11] to describe our results

$$a = (r_1 + r_2 + r_3)/3$$

$$e_x = (r_2 - r_1)/\sqrt{2} \qquad (1)$$

$$e_y = (r_2 + r_1 - 2r_3)/\sqrt{6}$$

where r_1, r_2, and r_3 are the lengths of the three sides of the C_3 triangle. The variables given by (1) do not determine the orientation of the plane of the CH_2 fragments, but in this discussion, unless otherwise specified, these have been set to minimize the energies on one or the other of the surfaces for a given a, e_x, and e_y. For many purposes a polar version of (1) is useful.

$$e = (e_x^2 + e_y^2)^{1/2} = [(r_1 - r_2)^2 + (r_1 - r_3)^2 + (r_2 - r_3)^2]^{1/2}/\sqrt{3}$$

$$\phi = \tan^{-1}(e_y/e_x) \qquad (2)$$

The variable a is the arithmetic average of the triangle sides and is thus a measure of the overall size of the triangle. From (2) we see that the e is just the root-mean-square deviation of the triangle sides from one another and measures the "distance" from the equilateral geometry. Clearly, if $r_1 = r_2 = r_3$, $e = 0$. When $e > 0$ the ϕ coordinate determines both the orientation and the shape of distortion from the equilateral state. The values of ϕ = 30, 150, and 270° correspond to isosceles triangles for which one side is longer than the other two. The values ϕ = 90, 210, and 330° correspond to isosceles triangles for which one side is shorter than the other two. When $e > 0$ and ϕ is not one of the above six angles, we have a scalene triangle in which no two sides are equal. Figure 1 shows how the shape of a triangle depends upon the coordinates for the values a = 2.5 Å, e = 1.0 Å, and several values of ϕ.

Simple orbital theory predicts that $C_3H_6^+$ should be in a degenerate state in D_{3h} symmetry and should distort spontaneously from this geometry because of the linear Jahn–Teller effect, with

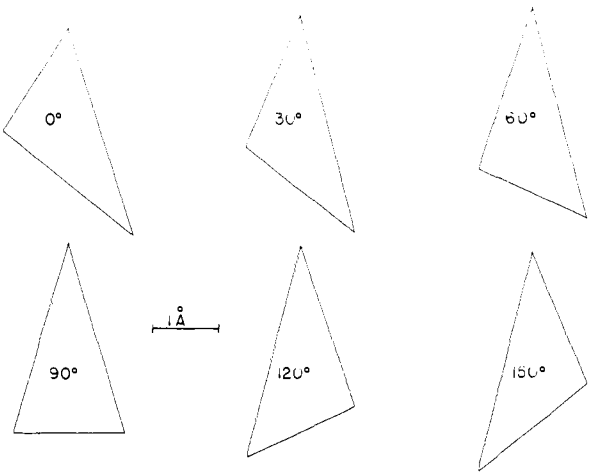

Figure 1. Illustration of the effect of the pseudorotation coordinate, ϕ, upon the shape of the triangle. These are shown for a = 2.5 Å and an e = 1.0 Å, with the 1-Å scale given.

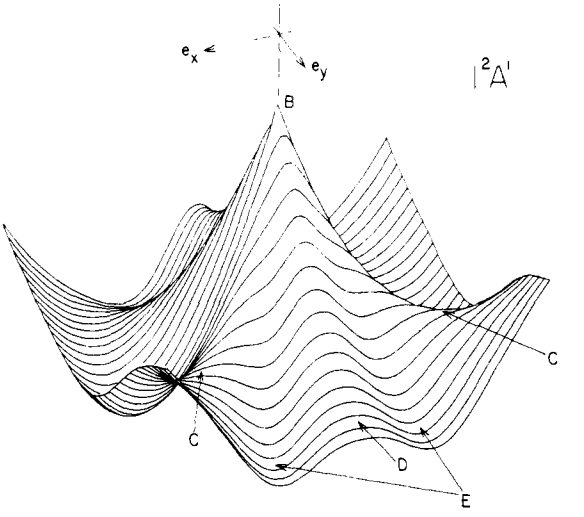

Figure 2. Three-dimensional representation of the lower $^2A'$ surface as a function of e_x and e_y for a constant a. The letters B, C, D, and E show points on the surface which are keyed to the energies and geometries displayed in Table I. This surface is plotted above the rectangle $-1.5 < e_x < 1.5$ and $-1.0 < e_y < 1.0$ in angstroms.

a splitting of the two degenerate states. Figure 2 gives a three-dimensional representation of the lower of these two surfaces as a function of $e_x$and e_y for a = 1.696 Å. We have expanded the vertical scale of Figure 2 so that the six equivalent minimum points which correspond to the six possible scalence triangles with sides 1.696, 1.860, and 1.532 Å are visible. There are three isosceles saddle points at ϕ = 90, 210, and 330°. These correspond to a chemical structure which is like a π complex of ethylene with a CH_2^+ as shown in I. There are three other isosceles saddle points

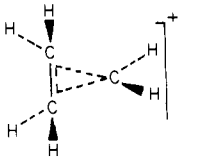

I

at ϕ = 30, 150, and 270°. These correspond to a chemical structure related to trimethylene with a one-electron bond for the long side as shown in II. The actual minima in the lower surface

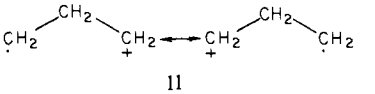

II

are approximately halfway between I and II. We will discuss

(10) J. J. C. Mulder, *Mol. Phys.*, **10**, 479 (1966); G. A. Gallup, *J. Chem. Phys.*, **50**, 1206 (1969); J. Paldus, *Ibid.*, **61**, 5321 (1974).
(11) R. L. Vance and G. A. Gallup, *J. Chem. Phys.*, **69**, 736 (1978).

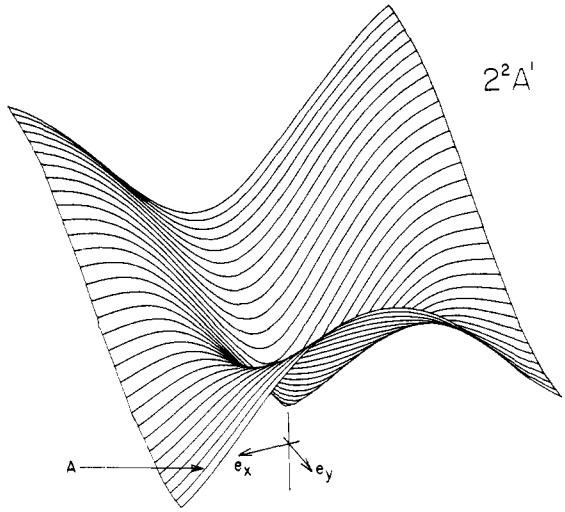

Figure 3. Three-dimensional representation o the upper $^2A'$ surface as a function of e_x and e_y for a constant a. The letters A and B are keyed to the energies and geometries given in Table I. This surface is plotted above the rectangle $-1.8 < e_x < 1.8$ and $-1.2 < e_y < 1.2$.

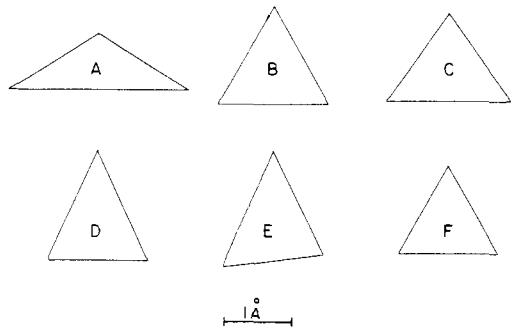

Figure 4. The six geometries of Table I shown in correct relative scale. The letters refer to the corresponding entries in Table I. The scale is 1 Å.

reasons for this distortion later.

The values of ϕ at which these six isosceles saddle points occur give the molecule C_{2v} symmetry, and at these angles C_{2v} symmetry classifications are valid. Thus for I we have a $^2B_2$ state and for II a $^2A_1$. (The C_2 axis of our C_{2v} group must rotate with ϕ, of course). We thus have a situation wherein the lower state may always be classified $^2A'$ in C_s symmetry, but as ϕ increases, the classification alternates between $^2A_1$ and $^2B_2$ at those critical angles for which the molecule is isosceles.

As ϕ changes along the minimal energy pseudorotation path with approximately constant a and e, the lower surface varies from top to bottom by 0.3 eV, the energy separation between the type II saddle point and the minimum scalene geometry.

The first excited $^2A'$ surface of $C_3H_6^+$ is shown in Figure 3, also in a three-dimensional representation. These results suggest that pseudorotation is unlikely in this state. The three minima are relatively deep and occur at ϕ = 30, 150, and 270°. These values for ϕ are, of course, C_{2v} symmetry points and the upper energy can here be classified as $^2B_2$. (We recall that the lower surface is $^2A_1$ at these angles.) The upper energy is, therefore, $^2A_1$ at ϕ = 90, 210, and 230°, where the lower surface is $^2B_2$.

We may summarize this behavior as follows: For values of $e \neq 0$, the first two surfaces are both, in general, $^2A'$ states, but as ϕ winds around, the upper and lower states alternate $^2A_1$ and $^2B_2$ character at those C_{2v} geometries where the C_3 triangle is isosceles.

The strong local minima in the upper surface are also versions of the trimethylene isomer II, but now with a one-electron *antibond* between the two open ends. This results in a much wider open version of the trimethylene radical ion than that found in the lower state. This effect is shown more clearly in Figure 5 which gives

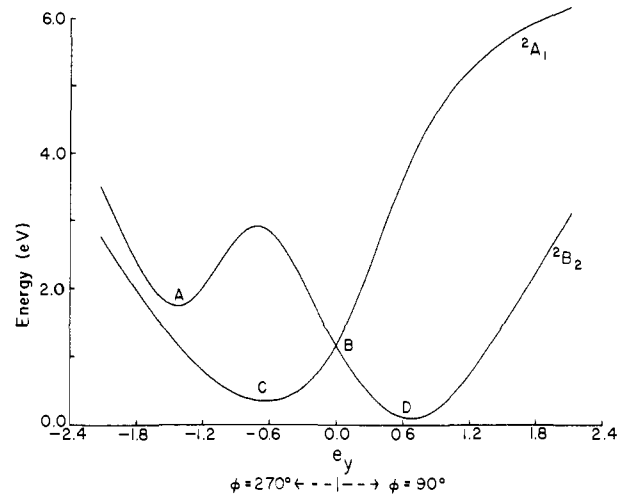

Figure 5. Intersection of the two surfaces with the $E - e_y$ plane. The letters refer to the energies and geometries in Table I.

Table I. Energies of Critical Geometries for C_3H_6 and $C_3H_6^+$

state	label[a]	R_1, Å	R_2, Å	R_3, Å	E au	E eV
$2^2A'$ min	A	1.592	1.592	2.715	−115.3062	10.9
$^2E'$ cusp	B	1.664	1.664	1.664	−115.3198	10.6
$1^2A'$ saddle	C	1.604	1.604	1.879	−115.3442	9.9
$1^2A'$ saddle	D	1.787	1.787	1.512	−115.3548	9.6
$1^2A'$ min	E	1.698	1.861	1.533	−115.3559	9.6
$^1A_1$ GC_3H_6	F	1.502[b]	1.502	1.502	−115.7076	0

[a] These letters are used to label points and diagrams on the figures. See figure captions for details. [b] Experimental.

the intersection of the E–e_y plane, with the two energy surfaces in correct relation to each other. Geometries with $e_y > 0$ correspond to cases where the unique angle of the triangle is <60° and $e_y < 0$ to cases where it is >60°.

We thus see that the lowest point on the lower energy surface corresponds to the chemical bonding structure halfway between I and II. The lowest point on the upper surface corresponds to resonating structure II with a one-electron antibond between the open ends and has $^2B_2$ symmetry.

Table I gives the energies and the geometries of these various minima and saddle points determined from analysis of functions fit to the calculated points. We label the states A–F in this table to key with various marked points in the figures. In Figure 4 we show the relative sizes and shapes of the C_3 triangle at these geometries.

For certain geometries the wagging angle of the CH_2 groups has a significant qualitative effect upon the energies. In the vicinity of structure II, the order of the energies $^2A_1$ and $^2B_2$ may be interchanged by changing the angle β defined in III. The $^2A_1$ state and $^2B_2$ states are expected to be influenced in opposite directions by changes in β. Examination of the signs of the

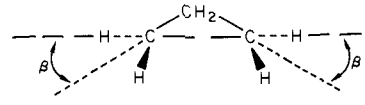

III

orbitals in III shows that the $^2A_1$ state should prefer small values of β since the $1b_2$ orbital on the central methylene cannot be singly occupied in this symmetry, and these same orbitals on the other two methylenes are pulled toward one another by the one-electron bond across the open side. For the $^2B_2$ state, the three $1b_2$ orbitals can interact with the outer lobes of opposite sign and hence push away from one another as part of the one-electron antibond across the open side. Changes in β will influence these interactions in different directions. When the $^2A_1$ and $^2B_2$ energies are close, as they are when the one-electron bond and antibond are extended,

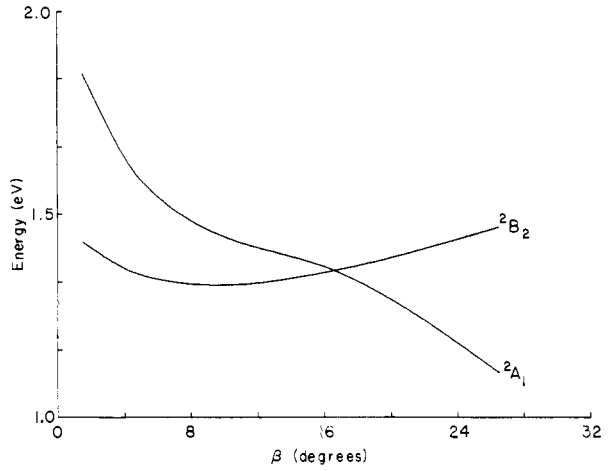

Figure 6. C_{2v} energies near structure II as functions of the CH_2 "wagging" angle, β. These curves are described more fully in the text.

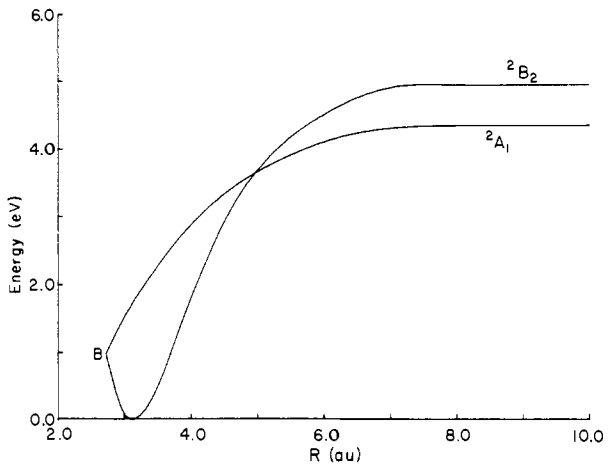

Figure 7. C_{2v} energies and the crossing for formation of $C_3H_6^+$ from $C_2H_4 + CH_2^+$ or $C_2H_4^+ + CH_2$. The point labeled as B refers to the energy and geometry in Table I.

the ordering of these two energies depends upon β. Figure 6 shows a graph of the energies in terms of β for a fixed triangle size.

The region of asymptotic separation of the C_2H_4 and CH_2 moieties is also of considerable interest for these surfaces, since a qualitative understanding of interactions here gives a rationale for the low symmetry of the absolute minimum geometry. Although the a, e, and ϕ coordinates could be used to describe these geometric arrangements, the set in IV is more convenient. When

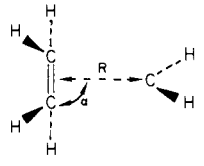

IV

$\alpha = \pi/2$ we have C_{2v} symmetry with C_s when $\alpha \neq \pi/2$. In the asymptotic region for C_{2v} geometries $C_2H_4 + CH_2^+$ is $^2A_1$ and $C_2H_4^+ + CH_2$ is $^2B_2$. The $^2A_1$ state is lower in energy since the ionization potential of methylene is smaller than that of ethylene. As the two atomic groups approach, the $^2B_2$ energy decreases more rapidly since both are open shell for this state. A C_{2v} curve crossing occurs at $R = 4.96$ au, and at shorter distances the $^2B_2$ state becomes more strongly bonding. We give a graph of these energies in Figure 7. If the same process were carried out for $\alpha \neq \pi/2$ the state crossing would be avoided since both states are then $^2A'$ and can interact. We therefore expect the energy of the lower $^2B_2$ state to be lowered even farther by distortions of α from $\pi/2$ and that this phenomenon will occur at least to some extent for all values of R smaller than the crossing. The possibility of interaction between these two states should therefore cause the absolute minimum to have low C_s rather than C_{2v} symmetry.

A mechanism like this does not operate for the upper surface at structures near II and the minimum there has a C_{2v} geometry.

Vibrational Structure of $C_3H_6^+$ and the PES of C_3H_6

In comparing these ab initio results with earlier semiempirical ones, we note first that we conclude that the C_3 triangle is rather more distorted from the equilateral at the bottom of the pseudorotation trough. The distortion may be expressed as e/a which is zero when $r_1 = r_2 = r_3$. The ab initio result for e/a is 0.137 while Rowland gets 0.097, some 30% smaller. In addition, the ab initio results indicate that $E_{^2B_2} < E_{^2A_1}$ while the CNDO gets the reverse order. Apparently semiempirical methods have never been used for C_s geometries to test whether still lower energies could be obtained by such procedures.

Along with discrepancies in these relatively small (with respect to energy differences) details, the ab initio calculations indicate a considerably greater complexity to these surfaces than the earlier semiempirical work has shown. This occurs particularly in the region of II where there is a strong local minimum in the upper surface, but the two energies interlace in a complicated fashion with respect to the CH_2 wagging angle.

As is seen in Table I the calculated separation between the $1^2A'$ minimum and the II geometry $2^2A'$ minimum is 1.3 eV. The closeness of this to the experimental separation of the peaks suggest that the two peaks in the PES of cyclopropane correspond to electronic transitions from the parent molecule to these two energy states of the ion. Since we expect a change in vibrational zero-point energy of less than 0.1 eV during this transition, the differences between our C_3H_6 energy and the energies for (approximately) I (lower surface) and II (upper surface) should correspond closely to the adiabatic onset of each of the PES peaks. According to the Frank–Condon principle, the low energy edge of a PES peak can be no lower than the adiabatic onset energy. Our values for the energy differences show good agreement with the experimental results[4] which lends support to this simple interpretation of the PES of C_3H_6.

Such a simple description of the physical process may be subjected to some criticism, the most serious probably being the observation that the rather great "distance" between the geometries of C_3H_6 and $2^2A'$ $C_3H_6^+$ (II) might prevent appreciable Frank–Condon intensity from showing for this configuration. However, further consideration leads one to see that both our original proposed mechanism and the criticism implicitly assume a good separation between electronic and vibrational motion near II. This is exceedingly unlikely. The penetration of the $2^2A'$ minima down into the pseudorotation trough and the crossing of levels with varying β suggest an incredibly complex vibronic mixing in these regions, with a consequent mixing of vibrational and electronic states which would produce the necessary Frank–Condon intensity. The vibronic interactions are also expected to produce a considerable change in the density of states approximately 1.3 eV above the ground state of $C_3H_6^+$, and we suggest that this change in density of states shows up as the double-peaked PES spectrum.

A complete modeling of the vibronic interactions here would require a treatment consisting of at least five vibrational coordinates, e, ϕ, and three βs, with a functional representation of the energies not restricted to the first few terms of a power series. Such a calculation represents a degree of complexity considerably beyond any so far carried out successfully.[12] And, indeed, this may be insufficient, since regions of the surfaces of lower than C_s symmetry are as yet unexplored. Further theoretical investigations of the PES spectrum appear to await the development of ability to handle these complex vibronic calculations.

Registry No. Cyclopropane radical cation, 34496-93-0; cyclopropane, 75-19-4.

(12) "The Jahn–Teller Effect in Molecules and Crystals", R. Englman, Wiley Interscience, New York, 1972; see, for example, E. R. Davidson and W. T. Borden, *J. Am. Chem. Soc.*, 99, 2053 (1977).